Measurement of CP violation in $B^0\rightarrow J/\psi K^0_\mathrm{S}$ and $B^0\rightarrow\psi(2S) K^0_\mathrm{S}$ decays

Published for SISSA by Springer

Received: *September 14, 2017*
Revised: *November 10, 2017*
Accepted: *November 12, 2017*
Published: *November 27, 2017*

Measurement of *CP* violation in $B^0 \to J/\psi\, K^0_S$ and $B^0 \to \psi(2S) K^0_S$ decays

The LHCb collaboration

E-mail: vanessa.mueller@cern.ch

Abstract: A measurement is presented of decay-time-dependent *CP* violation in the decays $B^0 \to J/\psi\, K^0_S$ and $B^0 \to \psi(2S) K^0_S$, where the J/ψ is reconstructed from two electrons and the $\psi(2S)$ from two muons. The analysis uses a sample of pp collision data recorded with the LHCb experiment at centre-of-mass energies of 7 and 8 TeV, corresponding to an integrated luminosity of $3\,\text{fb}^{-1}$. The *CP*-violation observables are measured to be

$$\begin{aligned} C\big(B^0 \to J/\psi\, K^0_S\big) &= 0.12 \pm 0.07 \pm 0.02\,, \\ S\big(B^0 \to J/\psi\, K^0_S\big) &= 0.83 \pm 0.08 \pm 0.01\,, \\ C\big(B^0 \to \psi(2S) K^0_S\big) &= -0.05 \pm 0.10 \pm 0.01\,, \\ S\big(B^0 \to \psi(2S) K^0_S\big) &= 0.84 \pm 0.10 \pm 0.01\,, \end{aligned}$$

where C describes *CP* violation in the direct decay, and S describes *CP* violation in the interference between the amplitudes for the direct decay and for the decay after B^0–$\overline{B}^0$ oscillation. The first uncertainties are statistical and the second are systematic. The two sets of results are compatible with the previous LHCb measurement using $B^0 \to J/\psi\, K^0_S$ decays, where the J/ψ meson was reconstructed from two muons. The averages of all three sets of LHCb results are

$$\begin{aligned} C(B^0 \to [c\bar{c}]K^0_S) &= -0.017 \pm 0.029\,, \\ S(B^0 \to [c\bar{c}]K^0_S) &= 0.760 \pm 0.034\,, \end{aligned}$$

under the assumption that higher-order contributions to the decay amplitudes are negligible. The uncertainties include statistical and systematic contributions.

Keywords: B physics, CKM angle beta, CP violation, Flavor physics, Hadron-Hadron scattering (experiments)

ArXiv ePrint: 1709.03944

https://doi.org/10.1007/JHEP11(2017)170

JHEP11(2017)170

Contents

1 Introduction 1

2 Detector and event selection 2

3 Invariant mass fit 4

4 Flavour tagging 5

5 *CP* asymmetry fit 6

6 Systematic uncertainties 8

7 Results and conclusion 8

The LHCb collaboration 13

1 Introduction

Precision measurements of CP violation in the decays of neutral B mesons provide stringent tests of the quark sector of the Standard Model (SM), in which CP violation arises due to a single irreducible phase of the Cabibbo-Kobayashi-Maskawa (CKM) quark-mixing matrix [1, 2]. The $B^0 \to [c\bar{c}]K^0_S$ family of decay modes, where $[c\bar{c}]$ denotes a charmonium resonance (J/ψ, $\psi(2S)$, η_c, *etc.*), is ideal for studying CP violation [3, 4]. Such decays proceed via a $b \to [c\bar{c}]s$ transition, where higher-order contributions that could introduce additional strong and weak phases in the decay amplitudes are expected to be small [5–7]. As B^0 and $\overline{B}^0$ mesons decay into a common final state in $B^0 \to [c\bar{c}]K^0_S$ decays,[1] the interference between the direct decay and decay after B^0–$\overline{B}^0$ mixing induces CP violation.

Since CP violation in the mixing is known to be negligible [8], the decay-time- and flavour-dependent decay rate for B^0 and $\overline{B}^0$ mesons can be expressed as

$$\Gamma(t,d) \propto \mathrm{e}^{-\frac{t}{\tau}}\Big[\cosh(\Delta\Gamma\, t/2) + A_{\Delta\Gamma}\sinh(\Delta\Gamma\, t/2) - d\cdot S\sin(\Delta m\, t) + d\cdot C\cos(\Delta m\, t)\Big]\,, \quad (1.1)$$

where in the equation the symbols are as follows: t is the proper decay time; τ is the mean lifetime of the B^0 and $\overline{B}^0$ meson; Δm and $\Delta\Gamma$ are the mass and decay width differences of the two B^0 mass eigenstates; d represents the B^0 meson flavour at production and takes

[1] The inclusion of charge-conjugate processes is implied throughout the article, unless otherwise noted. The notation B^0 refers to a neutral B meson containing a $\bar{b}$ and a d quark including the charge-conjugate state.

JHEP11(2017)170

values of $+1/-1$ for mesons with an initial flavour of $B^0/\overline{B}^0$; and S, C, and $A_{\Delta\Gamma}$ are the CP-violation observables. The asymmetry between the $\overline{B}^0$ and B^0 decay rates is given by

$$\begin{aligned}\mathcal{A}_{[c\overline{c}]K^0_S}(t) &\equiv \frac{\Gamma(\overline{B}^0(t)\to[c\overline{c}]K^0_S) - \Gamma(B^0(t)\to[c\overline{c}]K^0_S)}{\Gamma(\overline{B}^0(t)\to[c\overline{c}]K^0_S) + \Gamma(B^0(t)\to[c\overline{c}]K^0_S)} \\ &= \frac{S\sin(\Delta m\, t) - C\cos(\Delta m\, t)}{\cosh(\Delta\Gamma\, t/2) + A_{\Delta\Gamma}\sinh(\Delta\Gamma\, t/2)} \approx S\sin(\Delta m\, t) - C\cos(\Delta m\, t)\,,\end{aligned} \tag{1.2}$$

where the approximate expression is valid under the assumption $\Delta\Gamma = 0$, which is well motivated at the current experimental precision [8]. The observable C is related to CP violation in the direct decay, while the observable S corresponds to CP violation in the interference. The world average of $C = -0.004 \pm 0.015$ as given by the Heavy Flavor Averaging Group [8] is compatible with zero. The observable S can be written as a function of one of the angles of the unitarity triangle of the CKM matrix, $\beta \equiv \arg\left[-(V_{cd}V^*_{cb})/(V_{td}V^*_{tb})\right]$, which is the most precisely measured angle in the unitary triangle. In the limit of negligible higher-order contributions, which is assumed when combining results from different $B^0 \to [c\overline{c}]K^0_S$ modes, S can be identified as $\sin 2\beta$.

Applying CKM unitarity and using measurements of other CKM-related quantities leads to a SM prediction of $\sin 2\beta = 0.740^{+0.020}_{-0.025}$ by the CKMfitter group [9] and of $\sin 2\beta = 0.724 \pm 0.028$ by the UTfit collaboration [10]. The Belle and BaBar collaborations have already constrained $\sin 2\beta$ to a high precision in the $B^0 \to J/\psi\, K^0_S$ mode. They reported $S = 0.670 \pm 0.032$ [11] and $S = 0.657 \pm 0.038$ [12], respectively. The LHCb collaboration performed a measurement using $B^0 \to J/\psi\, K^0_S$ decays, where the J/ψ meson was reconstructed from two muons, and obtained a value of $S = 0.73 \pm 0.04$ [13].

This article presents a study of decay-time-dependent CP violation in the decays $B^0 \to J/\psi\, K^0_S$ and $B^0 \to \psi(2S)K^0_S$ using data collected with the LHCb experiment in pp collisions at centre-of-mass energies of 7 and 8 TeV, corresponding to a total integrated luminosity of $3\,\text{fb}^{-1}$. In both decays, only the $\pi^+\pi^-$ final state of the K^0_S meson is considered. The J/ψ meson is reconstructed from two electrons, whereas the $\psi(2S)$ is reconstructed from two muons. This is the first decay-time-dependent measurement at a hadron collider that uses electrons in the final state. Including these additional $B^0 \to [c\overline{c}]K^0_S$ decay modes results in a 20 % improvement in the precision on $\sin 2\beta$ at LHCb.

2 Detector and event selection

The LHCb detector [14, 15] is a single-arm forward spectrometer covering the pseudorapidity range from 2 to 5, designed for the study of particles containing b or c quarks. The detector includes a high-precision tracking system consisting of a silicon-strip vertex detector surrounding the pp interaction region, a large-area silicon-strip detector located upstream of a dipole magnet with a bending power of about 4 Tm, and three stations of silicon-strip detectors and straw drift tubes placed downstream of the magnet. The tracking system provides a measurement of momentum, p, of charged particles with a relative uncertainty that varies from 0.5% at low momentum to 1.0% at 200 GeV/c. The minimum distance of a track to a primary vertex, PV, the impact parameter, IP, is measured with

JHEP11(2017)170

a resolution of $(15 + 29/p_{\rm T})\,\mu$m, where $p_{\rm T}$ is the component of the momentum transverse to the beam, in GeV/c. Different types of charged hadrons are distinguished using information from two ring-imaging Cherenkov detectors. Photons, electrons, and hadrons are identified by a calorimeter system consisting of scintillating-pad and preshower detectors, an electromagnetic calorimeter, and a hadronic calorimeter. As bremsstrahlung from the electrons can significantly affect their momenta, a correction is applied using the measured momenta of photons associated to the electron. Muons are identified by a system composed of alternating layers of iron and multiwire proportional chambers.

The online event selection is performed by a trigger, which consists of a hardware stage, based on information from the calorimeter and muon systems, followed by a software stage, which applies a full event reconstruction. In the offline selection, trigger signals are associated with reconstructed particles. Selection requirements can therefore be made on the trigger selection itself and on whether the decision was due to the signal candidate, other particles produced in the pp collision, or a combination of both. While in the case of the J/ψ mode an inclusive approach is chosen to keep any candidate that passes both trigger stages, in the $\psi(2S)$ mode the muons can be used in the decision of the trigger due to their clean signature in the detector. For the $\psi(2S)$ mode events are selected at the hardware stage that contain at least one muon with transverse momentum $p_{\rm T} > 1.48\,{\rm GeV}/c$ in the 7 TeV data or $p_{\rm T} > 1.76\,{\rm GeV}/c$ in the 8 TeV data. In the subsequent software stage events are required to contain either at least one muon with a transverse momentum $p_{\rm T} > 1.0\,{\rm GeV}/c$ and IP $> 100\,\mu$m with respect to all PVs in the event, or two oppositely charged muons with combined mass $m(\mu^+\mu^-) > 2.7\,{\rm GeV}/c$. Finally, the tracks of two muons are required to form a vertex that is significantly displaced from the PVs.

The selection strategies are similar for $B^0 \to J/\psi\, K^0_{\rm S}$ and $B^0 \to \psi(2S) K^0_{\rm S}$ candidates. The B^0 candidates are reconstructed by combining charmonium and $K^0_{\rm S}$ candidates that form a common vertex. The charmonium candidates are formed from two oppositely charged tracks identified as electrons or muons. The pairs of tracks need to be of good quality and must form a vertex that is significantly displaced from any primary vertex. The muon candidates are required to have momenta $p > 8\,{\rm GeV}/c$ and transverse momenta $p_{\rm T} > 1\,{\rm GeV}/c$, and the dimuon invariant mass is in the range $3626 < m(\mu^+\mu^-) < 3746\,{\rm MeV}/c^2$. The electron candidates are required to have a $p_{\rm T} > 500\,{\rm MeV}/c$ and $2300 < m(e^+e^-) < 4000\,{\rm MeV}/c^2$, where a wider range compared to the dimuon mode is chosen to account for the worse resolution due to bremsstrahlung. The decay vertex of the $K^0_{\rm S}$ candidates must be significantly displaced from any PV, while the dipion invariant mass needs to be consistent with the known $K^0_{\rm S}$ mass [16].

The invariant mass of each B^0 candidate is determined by a kinematic fit [17], where the masses of the lepton and pion pairs are constrained to the known charmonium and $K^0_{\rm S}$ masses, respectively. The mass of the B^0 candidates is required to be in the range $5150 < m(J/\psi\, K^0_{\rm S}) < 5600\,{\rm MeV}/c^2$ or $5200 < m(\psi(2S) K^0_{\rm S}) < 5450\,{\rm MeV}/c^2$. The reconstructed decay time of the B^0 candidates, t', is obtained from a separate fit that constrains the B^0 candidate to originate from a PV. The B^0 candidates are kept if they have kinematic fits of a good quality, measured decay times in the range $0.2 < t' < 15\,{\rm ps}$ and decay-time-uncertainty estimates $\sigma_t < 0.4\,{\rm ps}$.

JHEP11(2017)170

To suppress combinatorial background, a multivariate selection is applied for each mode in which a boosted decision tree (BDT) [18] is trained using the AdaBoost boosting algorithm [19]. The BDTs are trained using simulated signal samples and background samples consisting of B^0 candidates with invariant masses above the considered regions, i.e. $5600 < m(J/\psi K^0_S) < 6000\,\mathrm{MeV}/c^2$ or $5450 < m(\psi(2S)K^0_S) < 5500\,\mathrm{MeV}/c^2$. The BDTs exploit features related to kinematic and topological properties of the decay, along with track- and vertex-reconstruction qualities. The common BDT features of the two decay modes are $p_\mathrm{T}(K^0_S)$, $p_\mathrm{T}([c\bar{c}])$, the χ^2 values of the kinematic fits, and the minimum and maximum of $\log(\chi^2_\mathrm{IP})$ for each pion and for each lepton, where χ^2_IP is defined as the increase in χ^2 when including the track in the PV fit. In addition to the common variables, the BDT for the J/ψ mode includes $p_\mathrm{T}(B^0)$, $\chi^2_\mathrm{IP}(J/\psi)$, $\chi^2_\mathrm{IP}(K^0_S)$, and the B^0-decay vertex-fit quality, $\chi^2_\mathrm{vtx}(B^0)$. The BDT for the $\psi(2S)$ mode includes $\chi^2_\mathrm{vtx}(K^0_S)$, and the K^0_S decay-time significance, $t/\sigma_t(K^0_S)$. The requirements on the BDT responses are chosen to maximise the expected sensitivity on the *CP* observable S.

To suppress possible contamination from $\Lambda^0_b \to [c\bar{c}]\Lambda(p\pi^-)$ decays, the dipion invariant mass is calculated under the $p\pi$ invariant mass hypothesis. Candidates compatible with the known Λ mass [16] are rejected. In the case of the J/ψ mode an additional proton-identification veto is applied. Aside from irreducible $B^0_s \to [c\bar{c}]K^0_S$ components that are modelled in the invariant mass fit, no other contributing peaking backgrounds are found.

Multiple combinations of B^0 candidates and PVs can occur in one event. After applying all selection criteria less than 1 % and 1.7 % multiple candidates are observed in the J/ψ and $\psi(2S)$ mode, respectively. Of these remaining multiple (B^0, PV) pairs per event, one is chosen randomly.

3 Invariant mass fit

Unbinned maximum likelihood fits to the invariant mass distributions, $m(J/\psi K^0_S)$ and $m(\psi(2S)K^0_S)$, are performed to determine signal candidate weights using the *sPlot* technique [20]. These signal candidate weights are used to statistically subtract the background in the *CP* asymmetry fit. The probability density functions (PDFs) of the signal and the $B^0_s \to [c\bar{c}]K^0_S$ background components are both parametrised by Hypatia functions [21], which consist of hyperbolic cores and power-law tails. The values of the parameters describing the tails are taken from simulation and used for both components. The widths of both components and the mean of the B^0 component are allowed to vary in the fit, while the mean of the B^0_s component is offset from the B^0 mean by the known B^0_s–B^0 mass difference [16]. The combinatorial background is described by an exponential function. The invariant mass distributions and the fit results are shown in figure 1. The fits yield a total of 10 630(140) $B^0 \to J/\psi K^0_S$ decays and 7970(100) $B^0 \to \psi(2S)K^0_S$ decays with mass resolutions of about $29\,\mathrm{MeV}/c^2$ and $7\,\mathrm{MeV}/c^2$, respectively. The worse resolution for the J/ψ mode is caused by the energy loss of the final state electrons, which cannot fully be corrected in the reconstruction.

JHEP11(2017)170

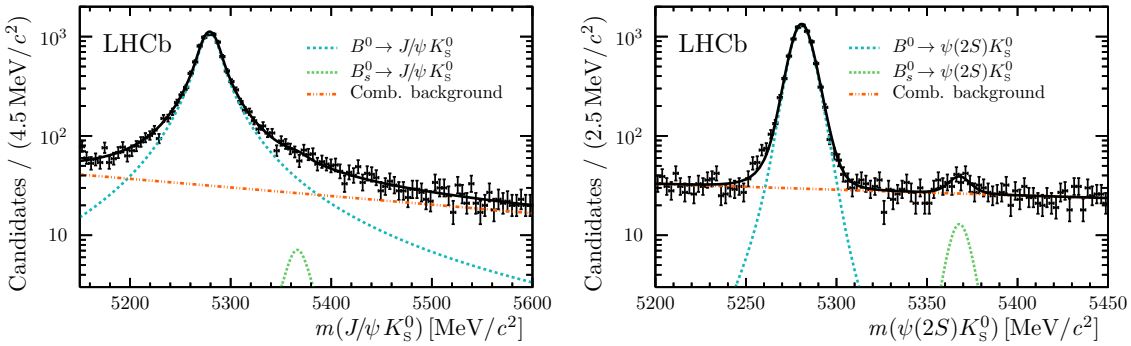

Figure 1. Invariant mass of the B^0 candidates for (left) the J/ψ and (right) the $\psi(2S)$ mode. The lines represent the result of the fit described in the text.

4 Flavour tagging

In a decay-time-dependent *CP*-violation measurement, it is essential to know the flavour of each B^0 meson at production. Multiple flavour-tagging algorithms are combined to achieve the best response. Each tagging algorithm provides a decision (tag), $d' \in \{-1, 0, 1\}$, corresponding to a B^0 candidate tagged as $\overline{B}^0$, untagged or tagged as B^0, respectively, and the mistag probability estimate, η. The tagging algorithms are categorised as same-side, SS, and opposite-side, OS [22–24]. The SS taggers exploit particles created in the fragmentation process of the B^0 meson, while the OS taggers use decay products of the accompanying b hadron that is produced in association with the signal B^0 meson.

The combination of OS taggers used in this analysis is based on different possible final states in the decay of the other b hadron in the event. The tagging responses are determined from the charges of muons, electrons or kaons; a weighted average of the charges of all tracks; and the decay products of charm decays possibly originating from the other b hadron in the event. In the case of the SS taggers the tagging decision is based on the charges of the pions and the protons originating from the fragmentation process of the signal B^0 mesons. The OS and SS decisions, $d'_{\rm OS}$ and $d'_{\rm SS}$, and their mistag estimates, $\eta_{\rm OS}$ and $\eta_{\rm SS}$, are combined for each B^0 candidate. The tags $d'_{\rm OS}$ and $d'_{\rm SS}$ are combined event-by-event during the fit procedure, taking into account their per-candidate mistag estimates.

The mistag estimates are calibrated using flavour-specific channels that are kinematically similar to the signal channels, so that η on average matches the signal mistag probability, $\omega(\eta)$. The difference in the tagging response for B^0 and $\overline{B}^0$ mesons is taken into account. The calibration channels are $B^+ \to J/\psi K^+$ for the OS taggers, and $B^0 \to J/\psi K^{*0}$ for the SS taggers, where the J/ψ is either reconstructed from two electrons or two muons. Selection criteria similar to the signal requirements are applied and signal candidate weights to subtract backgrounds are determined by a fit to the B^0 invariant masses, $m([c\overline{c}]K^+)$ and $m([c\overline{c}]K^{*0})$, with the *sPlot* technique. Before calibrating the tagging output the samples are weighted such that the relevant candidate kinematic distributions and properties match those of the signal decay. These distributions and properties are the pseudorapidity, the $p_{\rm T}(B^0)$, the number of tracks and primary vertices, and the azimuthal angle.

JHEP11(2017)170

Tagger	$B^0 \to J/\psi K^0_S$	$B^0 \to \psi(2S) K^0_S$
OS	3.60(13)	2.46(5)
SS	2.40(28)	1.07(8)
OS + SS	5.93(29)	3.42(9)

Table 1. Effective flavour-tagging efficiencies in per cent of the SS and OS taggers and their combination.

The effective tagging efficiency, $\varepsilon_{\rm eff} = \varepsilon_{\rm tag}\langle\mathcal{D}(\eta)^2\rangle$, is a measure of the effective statistical power of a data sample. Here, $\varepsilon_{\rm tag}$ is the tagging efficiency, defined as the fraction of candidates with a nonzero tag decision, and $\langle\mathcal{D}(\eta)^2\rangle$ is the effective dilution arising from the per-event dilution $\mathcal{D}(\eta) \equiv 1 - 2\omega(\eta)$. The effective tagging efficiencies for the OS and SS taggers and their combination are listed in table 1. A higher effective tagging efficiency in the J/ψ channel compared to the $\psi(2S)$ mode is observed for both the SS and OS flavour tagging. While the SS taggers are positively affected by a higher average $p_{\rm T}(B^0)$, the OS taggers benefit from the more inclusive trigger strategy in the J/ψ mode leading to lower mistag probabilities as well as higher tagging efficiencies in this mode.

5 *CP* asymmetry fit

The *CP* observables are determined by using an unbinned weighted maximum likelihood fit to the decay-time distributions for all $B^0 \to J/\psi K^0_S$ and $B^0 \to \psi(2S) K^0_S$ candidates. The signal candidate weights are determined from the mass fits described previously and used to subtract the background so that only the signal components need to be modelled. The PDF, $\mathcal{P}(t', \vec{d}' \,|\sigma_t, \vec{\eta})$, describes the measured B^0 candidate decay time and tags, $\vec{d}' = (d'_{\rm OS}, d'_{\rm SS})$. It also depends on the per-candidate decay-time-uncertainty estimate, σ_t, and the mistag probability estimates, $\vec{\eta} = (\eta_{\rm OS}, \eta_{\rm SS})$.

The fit is performed simultaneously in both decay modes, sharing the parameters describing the B^0 system, i.e. the B^0 meson lifetime, τ, and the mass difference, Δm, but allowing for different *CP* observables. The decay-time distribution of the signal components, $\mathcal{P}_{CP}(t, \vec{d}' \,|\vec{\eta})$, is derived from eq. (1.1) considering the production asymmetry, A_P, between $\overline{B}^0$ and B^0 mesons [25]. Using a PDF, $\mathcal{P}_{\rm tag}(\vec{d}' \,|d, \vec{\eta})$, which describes the distribution of tags based on the true production flavour and taking into account the mistag probability estimates and efficiencies, leads to

$$\mathcal{P}_{CP}(t, \vec{d}' \,|\vec{\eta}) \propto \sum_d \mathcal{P}_{\rm tag}(\vec{d}' \,|d, \vec{\eta})\,[1 - d \cdot A_{\rm P}]\, e^{-t/\tau}\{1 - d \cdot S \sin(\Delta m t) + d \cdot C \cos(\Delta m t)\}\,. \tag{5.1}$$

The decay-time resolution is taken into account by convolving $\mathcal{P}_{CP}$ with a resolution function, $\mathcal{R}(t' - t|\sigma_t)$. Furthermore, the decay-time distribution is multiplied by a decay-time-dependent reconstruction efficiency function, $\varepsilon(t')$, in order to take into account the distortion coming from the event reconstruction and selection. These corrections lead to

JHEP11(2017)170

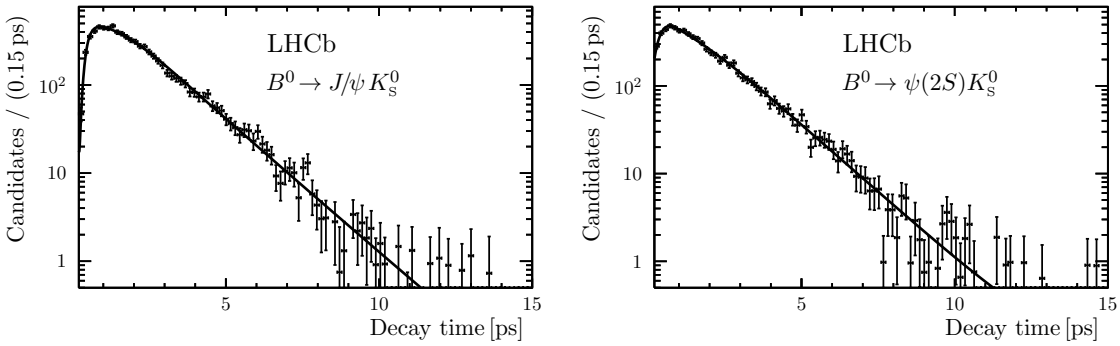

Figure 2. Projections of the decay-time fit to weighted (left) $B^0 \to J/\psi K^0_S$ and (right) $B^0 \to \psi(2S) K^0_S$ candidates.

the experimental decay-time distribution

$$\mathcal{P}\left(t', \vec{d}' \,|\sigma_t, \vec{\eta}\right) \propto \left(\mathcal{P}_{CP}(t, \vec{d}' \,|\vec{\eta}) \otimes \mathcal{R}(t' - t|\sigma_t)\right) \times \varepsilon(t')\,. \tag{5.2}$$

The resolution function is modelled by three Gaussian functions which describe the deviation of t' from t. The widths of two of these Gaussian functions are linear functions of σ_t and therefore vary for each candidate. The means are shared by all three Gaussians. The third Gaussian describes the proper-time resolution of candidates that have been associated with the wrong PV. The parameters of the resolution model are determined from simulated events and fixed in the fit, leading to effective single Gaussian resolutions of 67 fs for the J/ψ mode and 48 fs for the $\psi(2S)$ mode for correctly associated B^0 candidates. A small decay-time bias of 3 fs is observed in the simulation. This bias is neglected in the fit but is considered as a source of systematic uncertainty. The decay-time-dependent efficiency function is parametrized using cubic B-splines. The positions and the number of the knots for the splines are optimized on simulated data, whereas the coefficients are free fit parameters.

Potential differences between simulation and data are accounted for as systematic uncertainties. Production asymmetry values are evaluated for each mode and centre-of-mass energy, using the recent LHCb measurement [25] in bins of p_{T} and rapidity of the B^0 candidate. The values and uncertainties for the production asymmetry as well as for the external inputs for the B^0 system are listed in table 2. To propagate the uncertainties in the fit, these parameters and also the tagging-calibration parameters are Gaussian constrained using their statistical experimental uncertainties. Their systematic uncertainties, as well as the uncertainty due to the assumption $\Delta\Gamma = 0$, are accounted for in the systematic studies. Tagging-calibration parameters are constrained, taking into consideration their correlations. A fit validation using pseudoexperiments is performed, showing no bias and correctly estimated uncertainties from scans of the likelihood function [26]. The reconstructed decay-time distributions and the corresponding fit projections are shown in figure 2.

JHEP11(2017)170

Parameter	Value and uncertainty	Source
$A_{\rm P}^{7\,\rm TeV}(J/\psi)$	$-0.0100 \pm 0.0084 \pm 0.0005$	[25]
$A_{\rm P}^{8\,\rm TeV}(J/\psi)$	$-0.0077 \pm 0.0054 \pm 0.0004$	[25]
$A_{\rm P}^{7\,\rm TeV}(\psi(2S))$	$-0.0143 \pm 0.0077 \pm 0.0005$	[25]
$A_{\rm P}^{8\,\rm TeV}(\psi(2S))$	$-0.0138 \pm 0.0051 \pm 0.0003$	[25]
$\Delta m\,[\,\rm ps^{-1}]$	$0.5065 \pm 0.0016 \pm 0.0011$	[8]
τ[ps]	1.520 ± 0.004	[8]

Table 2. Parameters used as external inputs in the decay-time-dependent fit. The production asymmetries are evaluated individually for both decay modes and separately for the different centre-of-mass energies of 7 and 8 TeV. If two uncertainties are given the first is statistical and the second systematic. If one uncertainty is given it includes statistical and systematic contributions.

6 Systematic uncertainties

Systematic uncertainties arise due to possible mismodelling of the PDFs and from the uncertainties on the external inputs. The corresponding effects are studied using simulated pseudoexperiments in which ensembles are generated using parameters that differ from those used in the nominal fit. The generated datasets are then fitted with the nominal model to test whether biases in the parameters of interest occur.

The effect of neglecting $\Delta\Gamma$ in the nominal model is studied by varying its value within one standard deviation of its current experimental uncertainty [8]. Effects coming from the constrained inputs are evaluated by varying their values by one standard deviation in terms of their systematic experimental uncertainties. The constrained inputs are the production asymmetry parameters, the oscillation frequency, Δm, the lifetime, τ, as well as the tagging-calibration parameters. The systematic uncertainty arising due to the decay-time bias is evaluated using pseudoexperiments in which a corresponding value of 3 fs is assumed. Furthermore, deviations in the scaling of σ_t are estimated at the level of $\pm 30\,\%$ and addressed through varying the corresponding factors by this amount. Possible inaccuracies in the decay-time-reconstruction efficiency are studied using a different parameterization obtained from data. Table 3 summarizes the results of these studies. The individual uncertainties are added in quadrature to obtain the overall systematic uncertainties.

The fit results are corrected for *CP* violation in K^0–$\overline{K}^0$ mixing and for the difference in the nuclear cross-sections in material between K^0 and $\overline{K}^0$ interactions [27]. The numerical values of these corrections are -0.003 (-0.004) for S and $+0.002$ $(+0.002)$ for C in the J/ψ $(\psi(2S))$ mode.

7 Results and conclusion

The analysis of 10 630(140) $B^0 \to J/\psi K^0_{\rm S}$ and 7970(100) $B^0 \to \psi(2S)K^0_{\rm S}$ decays, where the J/ψ is reconstructed from two electrons and the $\psi(2S)$ from two muons, in a sample

JHEP11(2017)170

Source	$B^0 \to J/\psi K^0_S$		$B^0 \to \psi(2S) K^0_S$	
	σ_S	σ_C	σ_S	σ_C
$\Delta\Gamma$	0.003	0.007	0.007	0.003
Δm	0.004	0.004	0.004	0.004
Production asymmetry	0.004	0.009	0.007	0.005
Tagging calibration	0.002	0.005	0.005	0.002
Decay-time bias	0.006	0.006	0.006	0.004
σ_t scaling	0.003	0.005	0.002	0.002
Decay-time efficiency	0.006	0.004	0.006	0.004
Total	0.011	0.016	0.014	0.010

Table 3. Systematic uncertainties for the *CP*-violation observables S and C.

corresponding to $3\,\text{fb}^{-1}$ of pp collision data results in the *CP*-violation observables

$$\begin{aligned} C\big(B^0 \to J/\psi K^0_S\big) &= 0.12 \pm 0.07 \pm 0.02\,, \\ S\big(B^0 \to J/\psi K^0_S\big) &= 0.83 \pm 0.08 \pm 0.01\,, \\ C\big(B^0 \to \psi(2S) K^0_S\big) &= -0.05 \pm 0.10 \pm 0.01\,, \\ S\big(B^0 \to \psi(2S) K^0_S\big) &= 0.84 \pm 0.10 \pm 0.01\,, \end{aligned}$$

with correlation coefficients between S and C of 0.46 and 0.48 for the J/ψ and the $\psi(2S)$ mode, respectively. The first uncertainties are statistical and the second are systematic. The signal yield asymmetries, $(N_{\overline{B}^0} - N_{B^0})/(N_{\overline{B}^0} + N_{B^0})$, as a function of decay time are shown in figure 3, where N_{B^0} ($N_{\overline{B}^0}$) is the number of decays with a B^0 ($\overline{B}^0$) flavour tag. The results for the electron and muon modes are compatible with each other and with the previous LHCb measurements using $B^0 \to J/\psi K^0_S$ decays of $S = 0.73 \pm 0.04$ and $C = -0.038 \pm 0.032$ [13], where the J/ψ is reconstructed from two muons.

Combinations are performed using two-dimensional likelihood scans (see figure 4) taking into account the correlations between the single measurements. The quoted uncertainties include statistical and systematic contributions. Combining the LHCb results for both J/ψ modes leads to

$$\begin{aligned} C(B^0 \to J/\psi K^0_S) &= -0.014 \pm 0.030\,, \\ S(B^0 \to J/\psi K^0_S) &= 0.75 \pm 0.04\,, \end{aligned}$$

with a correlation coefficient of 0.42. This combination is compatible within 1.9 standard deviations with the $B^0 \to J/\psi K^0_S$ average of the B-factories [8], while the result for the $\psi(2S)$ mode is compatible within 0.3 standard deviations with the $B^0 \to \psi(2S) K^0_S$ average of the B-factories [8]. Building an LHCb average using the results from all $B^0 \to [c\overline{c}] K^0_S$ modes, i.e. $B^0 \to J/\psi K^0_S$, where the J/ψ is either reconstructed from two muons or two electrons, and $B^0 \to \psi(2S) K^0_S$, the *CP*-violation observables are determined to be

$$\begin{aligned} C(B^0 \to [c\overline{c}] K^0_S) &= -0.017 \pm 0.029\,, \\ S(B^0 \to [c\overline{c}] K^0_S) &= 0.760 \pm 0.034\,, \end{aligned}$$

JHEP11(2017)170

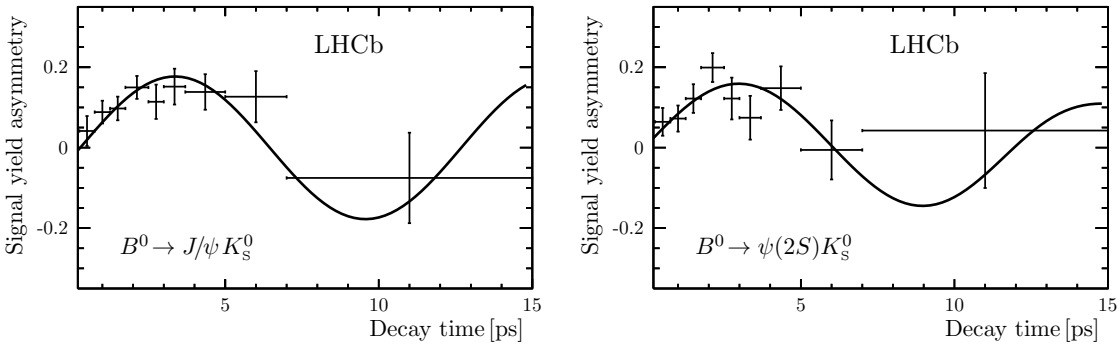

Figure 3. Signal yield asymmetries $(N_{\overline{B}^0} - N_{B^0})/(N_{\overline{B}^0} + N_{B^0})$ versus the decay time for (left) $B^0 \to J/\psi K^0_S$ and (right) $B^0 \to \psi(2S)K^0_S$ decays. The symbol N_{B^0} ($N_{\overline{B}^0}$) is the number of decays with a B^0 ($\overline{B}^0$) flavour tag. The solid curves are the projections of the PDF with the combined flavour tagging decision.

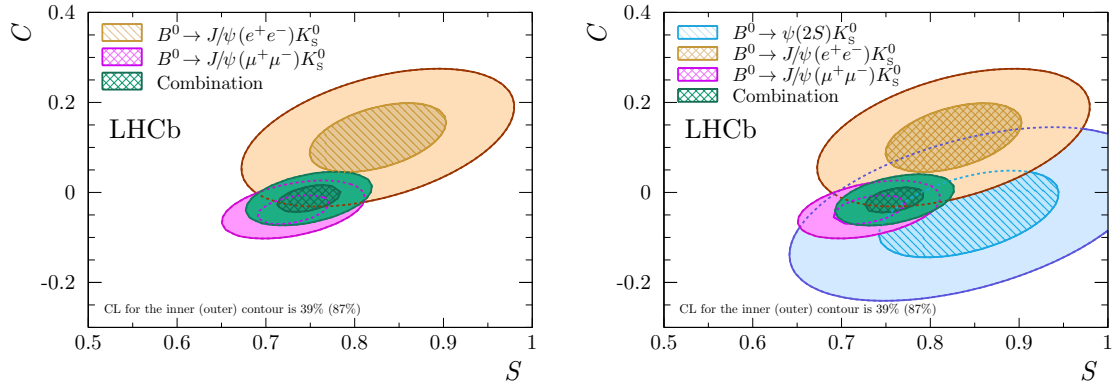

Figure 4. Two-dimensional likelihood scans for the combination of the (left) $B^0 \to J/\psi K^0_S$ modes and (right) all $B^0 \to [c\overline{c}]K^0_S$ modes. The confidence level for the inner (outer) contour is 39% (87%).

with a correlation coefficient of 0.42. These results are consistent with indirect measurements by the CKMfitter group [9] and the UTfit collaboration [10]. Furthermore, they improve the precision of $\sin 2\beta$ at LHCb by 20 %, and are expected to improve the precision of the world average.

Acknowledgments

We express our gratitude to our colleagues in the CERN accelerator departments for the excellent performance of the LHC. We thank the technical and administrative staff at the LHCb institutes. We acknowledge support from CERN and from the national agencies: CAPES, CNPq, FAPERJ and FINEP (Brazil); MOST and NSFC (China); CNRS/IN2P3 (France); BMBF, DFG and MPG (Germany); INFN (Italy); NWO (The Netherlands); MNiSW and NCN (Poland); MEN/IFA (Romania); MinES and FASO (Russia); MinECo (Spain); SNSF and SER (Switzerland); NASU (Ukraine); STFC (United Kingdom); NSF (U.S.A.). We acknowledge the computing resources that are provided by

JHEP11(2017)170

CERN, IN2P3 (France), KIT and DESY (Germany), INFN (Italy), SURF (The Netherlands), PIC (Spain), GridPP (United Kingdom), RRCKI and Yandex LLC (Russia), CSCS (Switzerland), IFIN-HH (Romania), CBPF (Brazil), PL-GRID (Poland) and OSC (U.S.A.). We are indebted to the communities behind the multiple open-source software packages on which we depend. Individual groups or members have received support from AvH Foundation (Germany), EPLANET, Marie Skłodowska-Curie Actions and ERC (European Union), ANR, Labex P2IO, ENIGMASS and OCEVU, and Région Auvergne-Rhône-Alpes (France), RFBR and Yandex LLC (Russia), GVA, XuntaGal and GENCAT (Spain), Herchel Smith Fund, the Royal Society, the English-Speaking Union and the Leverhulme Trust (United Kingdom).

References

[1] N. Cabibbo, *Unitary symmetry and leptonic decays*, *Phys. Rev. Lett.* **10** (1963) 531 [INSPIRE].

[2] M. Kobayashi and T. Maskawa, *CP violation in the renormalizable theory of weak interaction*, *Prog. Theor. Phys.* **49** (1973) 652 [INSPIRE].

[3] I.I.Y. Bigi and A.I. Sanda, *Notes on the observability of CP-violations in B decays*, *Nucl. Phys.* **B 193** (1981) 85 [INSPIRE].

[4] A.B. Carter and A.I. Sanda, *CP violation in B meson decays*, *Phys. Rev.* **D 23** (1981) 1567 [INSPIRE].

[5] S. Faller, M. Jung, R. Fleischer and T. Mannel, *The golden modes $B^0 \to J/\psi\, K^0_{S,L}$ in the era of precision flavour physics*, *Phys. Rev.* **D 79** (2009) 014030 [arXiv:0809.0842] [INSPIRE].

[6] M. Jung, *Determining weak phases from $B \to J/\psi P$ decays*, *Phys. Rev.* **D 86** (2012) 053008 [arXiv:1206.2050] [INSPIRE].

[7] P. Frings, U. Nierste and M. Wiebusch, *Penguin contributions to CP phases in $B_{d,s}$ decays to charmonium*, *Phys. Rev. Lett.* **115** (2015) 061802 [arXiv:1503.00859] [INSPIRE].

[8] Y. Amhis et al., *Averages of b-hadron, c-hadron and τ-lepton properties as of summer 2016*, arXiv:1612.07233 [INSPIRE]; updated results and plots available at http://www.slac.stanford.edu/xorg/hflav/.

[9] J. Charles et al., *Current status of the standard model CKM fit and constraints on $\Delta F = 2$ new physics*, *Phys. Rev.* **D 91** (2015) 073007 [arXiv:1501.05013] [INSPIRE]; updated results and plots available at http://ckmfitter.in2p3.fr/.

[10] UTfit collaboration, M. Bona et al., *The unitarity triangle fit in the standard model and hadronic parameters from lattice QCD: a reappraisal after the measurements of $\Delta m(s)$ and* BR$(B \to \tau\nu_\tau)$, *JHEP* **10** (2006) 081 [hep-ph/0606167] [INSPIRE]; updated results and plots available at http://www.utfit.org/.

[11] I. Adachi et al., *Precise measurement of the CP-violation parameter* $\sin(2\phi_1)$ *in $B^0 \to (c\bar{c})K^0$ decays*, *Phys. Rev. Lett.* **108** (2012) 171802 [arXiv:1201.4643] [INSPIRE].

JHEP11(2017)170

[12] BaBar collaboration, B. Aubert et al., *Measurement of time-dependent CP asymmetry in $B^0 \to c\bar{c}K^{(*)0}$ decays*, *Phys. Rev.* **D 79** (2009) 072009 [arXiv:0902.1708] [INSPIRE].

[13] LHCb collaboration, *Measurement of CP violation in $B^0 \to J/\psi K^0_S$ decays*, *Phys. Rev. Lett.* **115** (2015) 031601 [arXiv:1503.07089] [INSPIRE].

[14] LHCb collaboration, *The LHCb Detector at the LHC*, 2008 *JINST* **3** S08005 [INSPIRE].

[15] LHCb collaboration, *LHCb detector performance*, *Int. J. Mod. Phys.* **A 30** (2015) 1530022 [arXiv:1412.6352] [INSPIRE].

[16] Particle Data Group collaboration, C. Patrignani et al., *Review of particle physics*, *Chin. Phys.* **C 40** (2016) 100001 [INSPIRE]; and 2017 update.

[17] W.D. Hulsbergen, *Decay chain fitting with a Kalman filter*, *Nucl. Instrum. Meth.* **A 552** (2005) 566 [physics/0503191] [INSPIRE].

[18] F. Pedregosa et al., *Scikit-learn: machine learning in Python*, *J. Machine Learning Res.* **12** (2011) 2825 [arXiv:1201.0490] [INSPIRE].

[19] Y. Freund and R.E. Schapire, *A decision-theoretic generalization of on-line learning and an application to boosting*, *J. Comput. Syst. Sci.* **55** (1997) 119.

[20] M. Pivk and F.R. Le Diberder, *SPlot: a statistical tool to unfold data distributions*, *Nucl. Instrum. Meth.* **A 555** (2005) 356 [physics/0402083] [INSPIRE].

[21] D. Martínez Santos and F. Dupertuis, *Mass distributions marginalized over per-event errors*, *Nucl. Instrum. Meth.* **A 764** (2014) 150 [arXiv:1312.5000] [INSPIRE].

[22] LHCb collaboration, *Opposite-side flavour tagging of B mesons at the LHCb experiment*, *Eur. Phys. J.* **C 72** (2012) 2022 [arXiv:1202.4979] [INSPIRE].

[23] LHCb collaboration, *New algorithms for identifying the flavour of B^0 mesons using pions and protons*, *Eur. Phys. J.* **C 77** (2017) 238 [arXiv:1610.06019] [INSPIRE].

[24] LHCb collaboration, *B flavour tagging using charm decays at the LHCb experiment*, 2015 *JINST* **10** P10005 [arXiv:1507.07892] [INSPIRE].

[25] LHCb collaboration, *Measurement of B^0, B^0_s, B^+ and Λ^0_b production asymmetries in 7 and 8 TeV proton-proton collisions*, *Phys. Lett.* **B 774** (2017) 139 [arXiv:1703.08464] [INSPIRE].

[26] F. James and M. Roos, *Minuit: a system for function minimization and analysis of the parameter errors and correlations*, *Comput. Phys. Commun.* **10** (1975) 343 [INSPIRE].

[27] B.R. Ko, E. Won, B. Golob and P. Pakhlov, *Effect of nuclear interactions of neutral kaons on CP asymmetry measurements*, *Phys. Rev.* **D 84** (2011) 111501 [arXiv:1006.1938] [INSPIRE].

JHEP11(2017)170

The LHCb collaboration

R. Aaij[40], B. Adeva[39], M. Adinolfi[48], Z. Ajaltouni[5], S. Akar[59], J. Albrecht[10], F. Alessio[40], M. Alexander[53], A. Alfonso Albero[38], S. Ali[43], G. Alkhazov[31], P. Alvarez Cartelle[55], A.A. Alves Jr[59], S. Amato[2], S. Amerio[23], Y. Amhis[7], L. An[3], L. Anderlini[18], G. Andreassi[41], M. Andreotti[17,g], J.E. Andrews[60], R.B. Appleby[56], F. Archilli[43], P. d'Argent[12], J. Arnau Romeu[6], A. Artamonov[37], M. Artuso[61], E. Aslanides[6], G. Auriemma[26], M. Baalouch[5], I. Babuschkin[56], S. Bachmann[12], J.J. Back[50], A. Badalov[38,m], C. Baesso[62], S. Baker[55], V. Balagura[7,b], W. Baldini[17], A. Baranov[35], R.J. Barlow[56], C. Barschel[40], S. Barsuk[7], W. Barter[56], F. Baryshnikov[32], V. Batozskaya[29], V. Battista[41], A. Bay[41], L. Beaucourt[4], J. Beddow[53], F. Bedeschi[24], I. Bediaga[1], A. Beiter[61], L.J. Bel[43], N. Beliy[63], V. Bellee[41], N. Belloli[21,i], K. Belous[37], I. Belyaev[32,40], E. Ben-Haim[8], G. Bencivenni[19], S. Benson[43], S. Beranek[9], A. Berezhnoy[33], R. Bernet[42], D. Berninghoff[12], E. Bertholet[8], A. Bertolin[23], C. Betancourt[42], F. Betti[15], M.-O. Bettler[40], M. van Beuzekom[43], Ia. Bezshyiko[42], S. Bifani[47], P. Billoir[8], A. Birnkraut[10], A. Bizzeti[18,u], M. Bjørn[57], T. Blake[50], F. Blanc[41], S. Blusk[61], V. Bocci[26], T. Boettcher[58], A. Bondar[36,w], N. Bondar[31], I. Bordyuzhin[32], A. Borgheresi[21,i], S. Borghi[56], M. Borisyak[35], M. Borsato[39], F. Bossu[7], M. Boubdir[9], T.J.V. Bowcock[54], E. Bowen[42], C. Bozzi[17,40], S. Braun[12], T. Britton[61], J. Brodzicka[27], D. Brundu[16], E. Buchanan[48], C. Burr[56], A. Bursche[16,f], J. Buytaert[40], W. Byczynski[40], S. Cadeddu[16], H. Cai[64], R. Calabrese[17,g], R. Calladine[47], M. Calvi[21,i], M. Calvo Gomez[38,m], A. Camboni[38,m], P. Campana[19], D.H. Campora Perez[40], L. Capriotti[56], A. Carbone[15,e], G. Carboni[25,j], R. Cardinale[20,h], A. Cardini[16], P. Carniti[21,i], L. Carson[52], K. Carvalho Akiba[2], G. Casse[54], L. Cassina[21], M. Cattaneo[40], G. Cavallero[20,40,h], R. Cenci[24,t], D. Chamont[7], M.G. Chapman[48], M. Charles[8], Ph. Charpentier[40], G. Chatzikonstantinidis[47], M. Chefdeville[4], S. Chen[16], S.F. Cheung[57], S.-G. Chitic[40], V. Chobanova[39,40], M. Chrzaszcz[42,27], A. Chubykin[31], P. Ciambrone[19], X. Cid Vidal[39], G. Ciezarek[43], P.E.L. Clarke[52], M. Clemencic[40], H.V. Cliff[49], J. Closier[40], J. Cogan[6], E. Cogneras[5], V. Cogoni[16,f], L. Cojocariu[30], P. Collins[40], T. Colombo[40], A. Comerma-Montells[12], A. Contu[40], A. Cook[48], G. Coombs[40], S. Coquereau[38], G. Corti[40], M. Corvo[17,g], C.M. Costa Sobral[50], B. Couturier[40], G.A. Cowan[52], D.C. Craik[58], A. Crocombe[50], M. Cruz Torres[1], R. Currie[52], C. D'Ambrosio[40], F. Da Cunha Marinho[2], E. Dall'Occo[43], J. Dalseno[48], A. Davis[3], O. De Aguiar Francisco[40], S. De Capua[56], M. De Cian[12], J.M. De Miranda[1], L. De Paula[2], M. De Serio[14,d], P. De Simone[19], C.T. Dean[53], D. Decamp[4], L. Del Buono[8], H.-P. Dembinski[11], M. Demmer[10], A. Dendek[28], D. Derkach[35], O. Deschamps[5], F. Dettori[54], B. Dey[65], A. Di Canto[40], P. Di Nezza[19], H. Dijkstra[40], F. Dordei[40], M. Dorigo[40], A. Dosil Suárez[39], L. Douglas[53], A. Dovbnya[45], K. Dreimanis[54], L. Dufour[43], G. Dujany[8], P. Durante[40], R. Dzhelyadin[37], M. Dziewiecki[12], A. Dziurda[40], A. Dzyuba[31], S. Easo[51], M. Ebert[52], U. Egede[55], V. Egorychev[32], S. Eidelman[36,w], S. Eisenhardt[52], U. Eitschberger[10], R. Ekelhof[10], L. Eklund[53], S. Ely[61], S. Esen[12], H.M. Evans[49], T. Evans[57], A. Falabella[15], N. Farley[47], S. Farry[54], D. Fazzini[21,i], L. Federici[25], D. Ferguson[52], G. Fernandez[38], P. Fernandez Declara[40], A. Fernandez Prieto[39], F. Ferrari[15], F. Ferreira Rodrigues[2], M. Ferro-Luzzi[40], S. Filippov[34], R.A. Fini[14], M. Fiorini[17,g], M. Firlej[28], C. Fitzpatrick[41], T. Fiutowski[28], F. Fleuret[7,b], K. Fohl[40], M. Fontana[16,40], F. Fontanelli[20,h], D.C. Forshaw[61], R. Forty[40], V. Franco Lima[54], M. Frank[40], C. Frei[40], J. Fu[22,q], W. Funk[40], E. Furfaro[25,j], C. Färber[40], E. Gabriel[52], A. Gallas Torreira[39], D. Galli[15,e], S. Gallorini[23], S. Gambetta[52], M. Gandelman[2], P. Gandini[22], Y. Gao[3], L.M. Garcia Martin[70], J. García Pardiñas[39], J. Garra Tico[49], L. Garrido[38], P.J. Garsed[49], D. Gascon[38], C. Gaspar[40], L. Gavardi[10], G. Gazzoni[5], D. Gerick[12], E. Gersabeck[12], M. Gersabeck[56], T. Gershon[50], Ph. Ghez[4], S. Gianì[41], V. Gibson[49], O.G. Girard[41], L. Giubega[30], K. Gizdov[52], V.V. Gligorov[8], D. Golubkov[32],

JHEP11(2017)170

A. Golutvin[55], A. Gomes[1,a], I.V. Gorelov[33], C. Gotti[21,i], E. Govorkova[43], J.P. Grabowski[12], R. Graciani Diaz[38], L.A. Granado Cardoso[40], E. Graugés[38], E. Graverini[42], G. Graziani[18], A. Grecu[30], R. Greim[9], P. Griffith[16], L. Grillo[21], L. Gruber[40], B.R. Gruberg Cazon[57], O. Grünberg[67], E. Gushchin[34], Yu. Guz[37], T. Gys[40], C. Göbel[62], T. Hadavizadeh[57], C. Hadjivasiliou[5], G. Haefeli[41], C. Haen[40], S.C. Haines[49], B. Hamilton[60], X. Han[12], T.H. Hancock[57], S. Hansmann-Menzemer[12], N. Harnew[57], S.T. Harnew[48], C. Hasse[40], M. Hatch[40], J. He[63], M. Hecker[55], K. Heinicke[10], A. Heister[9], K. Hennessy[54], P. Henrard[5], L. Henry[70], E. van Herwijnen[40], M. Heß[67], A. Hicheur[2], D. Hill[57], C. Hombach[56], P.H. Hopchev[41], W. Hu[65], Z.C. Huard[59], W. Hulsbergen[43], T. Humair[55], M. Hushchyn[35], D. Hutchcroft[54], P. Ibis[10], M. Idzik[28], P. Ilten[58], R. Jacobsson[40], J. Jalocha[57], E. Jans[43], A. Jawahery[60], F. Jiang[3], M. John[57], D. Johnson[40], C.R. Jones[49], C. Joram[40], B. Jost[40], N. Jurik[57], S. Kandybei[45], M. Karacson[40], J.M. Kariuki[48], S. Karodia[53], N. Kazeev[35], M. Kecke[12], M. Kelsey[61], M. Kenzie[49], T. Ketel[44], E. Khairullin[35], B. Khanji[12], C. Khurewathanakul[41], T. Kirn[9], S. Klaver[56], K. Klimaszewski[29], T. Klimkovich[11], S. Koliiev[46], M. Kolpin[12], I. Komarov[41], R. Kopecna[12], P. Koppenburg[43], A. Kosmyntseva[32], S. Kotriakhova[31], M. Kozeiha[5], L. Kravchuk[34], M. Kreps[50], F. Kress[55], P. Krokovny[36,w], F. Kruse[10], W. Krzemien[29], W. Kucewicz[27,l], M. Kucharczyk[27], V. Kudryavtsev[36,w], A.K. Kuonen[41], T. Kvaratskheliya[32,40], D. Lacarrere[40], G. Lafferty[56], A. Lai[16], G. Lanfranchi[19], C. Langenbruch[9], T. Latham[50], C. Lazzeroni[47], R. Le Gac[6], A. Leflat[33,40], J. Lefrançois[7], R. Lefèvre[5], F. Lemaitre[40], E. Lemos Cid[39], O. Leroy[6], T. Lesiak[27], B. Leverington[12], P.-R. Li[63], T. Li[3], Y. Li[7], Z. Li[61], T. Likhomanenko[68], R. Lindner[40], F. Lionetto[42], V. Lisovskyi[7], X. Liu[3], D. Loh[50], A. Loi[16], I. Longstaff[53], J.H. Lopes[2], D. Lucchesi[23,o], M. Lucio Martinez[39], H. Luo[52], A. Lupato[23], E. Luppi[17,g], O. Lupton[40], A. Lusiani[24], X. Lyu[63], F. Machefert[7], F. Maciuc[30], V. Macko[41], P. Mackowiak[10], S. Maddrell-Mander[48], O. Maev[31,40], K. Maguire[56], D. Maisuzenko[31], M.W. Majewski[28], S. Malde[57], A. Malinin[68], T. Maltsev[36,w], G. Manca[16,f], G. Mancinelli[6], D. Marangotto[22,q], J. Maratas[5,v], J.F. Marchand[4], U. Marconi[15], C. Marin Benito[38], M. Marinangeli[41], P. Marino[41], J. Marks[12], G. Martellotti[26], M. Martin[6], M. Martinelli[41], D. Martinez Santos[39], F. Martinez Vidal[70], D. Martins Tostes[2], L.M. Massacrier[7], A. Massafferri[1], R. Matev[40], A. Mathad[50], Z. Mathe[40], C. Matteuzzi[21], A. Mauri[42], E. Maurice[7,b], B. Maurin[41], A. Mazurov[47], M. McCann[55,40], A. McNab[56], R. McNulty[13], J.V. Mead[54], B. Meadows[59], C. Meaux[6], F. Meier[10], N. Meinert[67], D. Melnychuk[29], M. Merk[43], A. Merli[22,40,q], E. Michielin[23], D.A. Milanes[66], E. Millard[50], M.-N. Minard[4], L. Minzoni[17], D.S. Mitzel[12], A. Mogini[8], J. Molina Rodriguez[1], T. Mombächer[10], I.A. Monroy[66], S. Monteil[5], M. Morandin[23], M.J. Morello[24,t], O. Morgunova[68], J. Moron[28], A.B. Morris[52], R. Mountain[61], F. Muheim[52], M. Mulder[43], D. Müller[56], J. Müller[10], K. Müller[42], V. Müller[10], P. Naik[48], T. Nakada[41], R. Nandakumar[51], A. Nandi[57], I. Nasteva[2], M. Needham[52], N. Neri[22,40], S. Neubert[12], N. Neufeld[40], M. Neuner[12], T.D. Nguyen[41], C. Nguyen-Mau[41,n], S. Nieswand[9], R. Niet[10], N. Nikitin[33], T. Nikodem[12], A. Nogay[68], D.P. O'Hanlon[50], A. Oblakowska-Mucha[28], V. Obraztsov[37], S. Ogilvy[19], R. Oldeman[16,f], C.J.G. Onderwater[71], A. Ossowska[27], J.M. Otalora Goicochea[2], P. Owen[42], A. Oyanguren[70], P.R. Pais[41], A. Palano[14,d], M. Palutan[19,40], A. Papanestis[51], M. Pappagallo[14,d], L.L. Pappalardo[17,g], W. Parker[60], C. Parkes[56], G. Passaleva[18,40], A. Pastore[14,d], M. Patel[55], C. Patrignani[15,e], A. Pearce[40], A. Pellegrino[43], G. Penso[26], M. Pepe Altarelli[40], S. Perazzini[40], P. Perret[5], L. Pescatore[41], K. Petridis[48], A. Petrolini[20,h], A. Petrov[68], M. Petruzzo[22,q], E. Picatoste Olloqui[38], B. Pietrzyk[4], M. Pikies[27], D. Pinci[26], F. Pisani[40], A. Pistone[20,h], A. Piucci[12], V. Placinta[30], S. Playfer[52], M. Plo Casasus[39], F. Polci[8], M. Poli Lener[19], A. Poluektov[50], I. Polyakov[61], E. Polycarpo[2], G.J. Pomery[48], S. Ponce[40], A. Popov[37], D. Popov[11,40], S. Poslavskii[37], C. Potterat[2], E. Price[48], J. Prisciandaro[39], C. Prouve[48], V. Pugatch[46], A. Puig Navarro[42], H. Pullen[57], G. Punzi[24,p],

JHEP11(2017)170

W. Qian[50], R. Quagliani[7,48], B. Quintana[5], B. Rachwal[28], J.H. Rademacker[48], M. Rama[24], M. Ramos Pernas[39], M.S. Rangel[2], I. Raniuk[45,†], F. Ratnikov[35], G. Raven[44], M. Ravonel Salzgeber[40], M. Reboud[4], F. Redi[55], S. Reichert[10], A.C. dos Reis[1], C. Remon Alepuz[70], V. Renaudin[7], S. Ricciardi[51], S. Richards[48], M. Rihl[40], K. Rinnert[54], V. Rives Molina[38], P. Robbe[7], A. Robert[8], A.B. Rodrigues[1], E. Rodrigues[59], J.A. Rodriguez Lopez[66], A. Rogozhnikov[35], S. Roiser[40], A. Rollings[57], V. Romanovskiy[37], A. Romero Vidal[39], J.W. Ronayne[13], M. Rotondo[19], M.S. Rudolph[61], T. Ruf[40], P. Ruiz Valls[70], J. Ruiz Vidal[70], J.J. Saborido Silva[39], E. Sadykhov[32], N. Sagidova[31], B. Saitta[16,f], V. Salustino Guimaraes[1], C. Sanchez Mayordomo[70], B. Sanmartin Sedes[39], R. Santacesaria[26], C. Santamarina Rios[39], M. Santimaria[19], E. Santovetti[25,j], G. Sarpis[56], A. Sarti[19,k], C. Satriano[26,s], A. Satta[25], D.M. Saunders[48], D. Savrina[32,33], S. Schael[9], M. Schellenberg[10], M. Schiller[53], H. Schindler[40], M. Schmelling[11], T. Schmelzer[10], B. Schmidt[40], O. Schneider[41], A. Schopper[40], H.F. Schreiner[59], M. Schubiger[41], M.-H. Schune[7], R. Schwemmer[40], B. Sciascia[19], A. Sciubba[26,k], A. Semennikov[32], E.S. Sepulveda[8], A. Sergi[47], N. Serra[42], J. Serrano[6], L. Sestini[23], A. Seuthe[10], P. Seyfert[40], M. Shapkin[37], I. Shapoval[45], Y. Shcheglov[31], T. Shears[54], L. Shekhtman[36,w], V. Shevchenko[68], B.G. Siddi[17], R. Silva Coutinho[42], L. Silva de Oliveira[2], G. Simi[23,o], S. Simone[14,d], M. Sirendi[49], N. Skidmore[48], T. Skwarnicki[61], E. Smith[55], I.T. Smith[52], J. Smith[49], M. Smith[55], l. Soares Lavra[1], M.D. Sokoloff[59], F.J.P. Soler[53], B. Souza De Paula[2], B. Spaan[10], P. Spradlin[53], S. Sridharan[40], F. Stagni[40], M. Stahl[12], S. Stahl[40], P. Stefko[41], S. Stefkova[55], O. Steinkamp[42], S. Stemmle[12], O. Stenyakin[37], M. Stepanova[31], H. Stevens[10], S. Stone[61], B. Storaci[42], S. Stracka[24,p], M.E. Stramaglia[41], M. Straticiuc[30], U. Straumann[42], J. Sun[3], L. Sun[64], W. Sutcliffe[55], K. Swientek[28], V. Syropoulos[44], T. Szumlak[28], M. Szymanski[63], S. T'Jampens[4], A. Tayduganov[6], T. Tekampe[10], G. Tellarini[17,g], F. Teubert[40], E. Thomas[40], J. van Tilburg[43], M.J. Tilley[55], V. Tisserand[4], M. Tobin[41], S. Tolk[49], L. Tomassetti[17,g], D. Tonelli[24], F. Toriello[61], R. Tourinho Jadallah Aoude[1], E. Tournefier[4], M. Traill[53], M.T. Tran[41], M. Tresch[42], A. Trisovic[40], A. Tsaregorodtsev[6], P. Tsopelas[43], A. Tully[49], N. Tuning[43,40], A. Ukleja[29], A. Usachov[7], A. Ustyuzhanin[35], U. Uwer[12], C. Vacca[16,f], A. Vagner[69], V. Vagnoni[15,40], A. Valassi[40], S. Valat[40], G. Valenti[15], R. Vazquez Gomez[19], P. Vazquez Regueiro[39], S. Vecchi[17], M. van Veghel[43], J.J. Velthuis[48], M. Veltri[18,r], G. Veneziano[57], A. Venkateswaran[61], T.A. Verlage[9], M. Vernet[5], M. Vesterinen[57], J.V. Viana Barbosa[40], B. Viaud[7], D. Vieira[63], M. Vieites Diaz[39], H. Viemann[67], X. Vilasis-Cardona[38,m], M. Vitti[49], V. Volkov[33], A. Vollhardt[42], B. Voneki[40], A. Vorobyev[31], V. Vorobyev[36,w], C. Voß[9], J.A. de Vries[43], C. Vázquez Sierra[39], R. Waldi[67], C. Wallace[50], R. Wallace[13], J. Walsh[24], J. Wang[61], D.R. Ward[49], H.M. Wark[54], N.K. Watson[47], D. Websdale[55], A. Weiden[42], C. Weisser[58], M. Whitehead[40], J. Wicht[50], G. Wilkinson[57], M. Wilkinson[61], M. Williams[56], M.P. Williams[47], M. Williams[58], T. Williams[47], F.F. Wilson[51,40], J. Wimberley[60], M. Winn[7], J. Wishahi[10], W. Wislicki[29], M. Witek[27], G. Wormser[7], S.A. Wotton[49], K. Wraight[53], K. Wyllie[40], Y. Xie[65], M. Xu[65], Z. Xu[4], Z. Yang[3], Z. Yang[60], Y. Yao[61], H. Yin[65], J. Yu[65], X. Yuan[61], O. Yushchenko[37], K.A. Zarebski[47], M. Zavertyaev[11,c], L. Zhang[3], Y. Zhang[7], A. Zhelezov[12], Y. Zheng[63], X. Zhu[3], V. Zhukov[33], J.B. Zonneveld[52], S. Zucchelli[15]

[1] *Centro Brasileiro de Pesquisas Físicas (CBPF), Rio de Janeiro, Brazil*
[2] *Universidade Federal do Rio de Janeiro (UFRJ), Rio de Janeiro, Brazil*
[3] *Center for High Energy Physics, Tsinghua University, Beijing, China*
[4] *LAPP, Université Savoie Mont-Blanc, CNRS/IN2P3, Annecy-Le-Vieux, France*
[5] *Clermont Université, Université Blaise Pascal, CNRS/IN2P3, LPC, Clermont-Ferrand, France*
[6] *Aix Marseille Univ, CNRS/IN2P3, CPPM, Marseille, France*
[7] *LAL, Université Paris-Sud, CNRS/IN2P3, Orsay, France*
[8] *LPNHE, Université Pierre et Marie Curie, Université Paris Diderot, CNRS/IN2P3, Paris, France*

JHEP11(2017)170

[9] I. Physikalisches Institut, RWTH Aachen University, Aachen, Germany
[10] Fakultät Physik, Technische Universität Dortmund, Dortmund, Germany
[11] Max-Planck-Institut für Kernphysik (MPIK), Heidelberg, Germany
[12] Physikalisches Institut, Ruprecht-Karls-Universität Heidelberg, Heidelberg, Germany
[13] School of Physics, University College Dublin, Dublin, Ireland
[14] Sezione INFN di Bari, Bari, Italy
[15] Sezione INFN di Bologna, Bologna, Italy
[16] Sezione INFN di Cagliari, Cagliari, Italy
[17] Universita e INFN, Ferrara, Ferrara, Italy
[18] Sezione INFN di Firenze, Firenze, Italy
[19] Laboratori Nazionali dell'INFN di Frascati, Frascati, Italy
[20] Sezione INFN di Genova, Genova, Italy
[21] Universita & INFN, Milano-Bicocca, Milano, Italy
[22] Sezione di Milano, Milano, Italy
[23] Sezione INFN di Padova, Padova, Italy
[24] Sezione INFN di Pisa, Pisa, Italy
[25] Sezione INFN di Roma Tor Vergata, Roma, Italy
[26] Sezione INFN di Roma La Sapienza, Roma, Italy
[27] Henryk Niewodniczanski Institute of Nuclear Physics Polish Academy of Sciences, Kraków, Poland
[28] AGH - University of Science and Technology, Faculty of Physics and Applied Computer Science, Kraków, Poland
[29] National Center for Nuclear Research (NCBJ), Warsaw, Poland
[30] Horia Hulubei National Institute of Physics and Nuclear Engineering, Bucharest-Magurele, Romania
[31] Petersburg Nuclear Physics Institute (PNPI), Gatchina, Russia
[32] Institute of Theoretical and Experimental Physics (ITEP), Moscow, Russia
[33] Institute of Nuclear Physics, Moscow State University (SINP MSU), Moscow, Russia
[34] Institute for Nuclear Research of the Russian Academy of Sciences (INR RAN), Moscow, Russia
[35] Yandex School of Data Analysis, Moscow, Russia
[36] Budker Institute of Nuclear Physics (SB RAS), Novosibirsk, Russia
[37] Institute for High Energy Physics (IHEP), Protvino, Russia
[38] ICCUB, Universitat de Barcelona, Barcelona, Spain
[39] Universidad de Santiago de Compostela, Santiago de Compostela, Spain
[40] European Organization for Nuclear Research (CERN), Geneva, Switzerland
[41] Institute of Physics, Ecole Polytechnique Fédérale de Lausanne (EPFL), Lausanne, Switzerland
[42] Physik-Institut, Universität Zürich, Zürich, Switzerland
[43] Nikhef National Institute for Subatomic Physics, Amsterdam, The Netherlands
[44] Nikhef National Institute for Subatomic Physics and VU University Amsterdam, Amsterdam, The Netherlands
[45] NSC Kharkiv Institute of Physics and Technology (NSC KIPT), Kharkiv, Ukraine
[46] Institute for Nuclear Research of the National Academy of Sciences (KINR), Kyiv, Ukraine
[47] University of Birmingham, Birmingham, United Kingdom
[48] H.H. Wills Physics Laboratory, University of Bristol, Bristol, United Kingdom
[49] Cavendish Laboratory, University of Cambridge, Cambridge, United Kingdom
[50] Department of Physics, University of Warwick, Coventry, United Kingdom
[51] STFC Rutherford Appleton Laboratory, Didcot, United Kingdom
[52] School of Physics and Astronomy, University of Edinburgh, Edinburgh, United Kingdom
[53] School of Physics and Astronomy, University of Glasgow, Glasgow, United Kingdom
[54] Oliver Lodge Laboratory, University of Liverpool, Liverpool, United Kingdom
[55] Imperial College London, London, United Kingdom
[56] School of Physics and Astronomy, University of Manchester, Manchester, United Kingdom
[57] Department of Physics, University of Oxford, Oxford, United Kingdom

JHEP11(2017)170

[58] Massachusetts Institute of Technology, Cambridge, MA, United States
[59] University of Cincinnati, Cincinnati, OH, United States
[60] University of Maryland, College Park, MD, United States
[61] Syracuse University, Syracuse, NY, United States
[62] Pontifícia Universidade Católica do Rio de Janeiro (PUC-Rio), Rio de Janeiro, Brazil, associated to[2]
[63] University of Chinese Academy of Sciences, Beijing, China, associated to[3]
[64] School of Physics and Technology, Wuhan University, Wuhan, China, associated to[3]
[65] Institute of Particle Physics, Central China Normal University, Wuhan, Hubei, China, associated to[3]
[66] Departamento de Fisica , Universidad Nacional de Colombia, Bogota, Colombia, associated to[8]
[67] Institut für Physik, Universität Rostock, Rostock, Germany, associated to[12]
[68] National Research Centre Kurchatov Institute, Moscow, Russia, associated to[32]
[69] National Research Tomsk Polytechnic University, Tomsk, Russia, associated to[32]
[70] Instituto de Fisica Corpuscular, Centro Mixto Universidad de Valencia - CSIC, Valencia, Spain, associated to[38]
[71] Van Swinderen Institute, University of Groningen, Groningen, The Netherlands, associated to[43]

[a] Universidade Federal do Triângulo Mineiro (UFTM), Uberaba-MG, Brazil
[b] Laboratoire Leprince-Ringuet, Palaiseau, France
[c] P.N. Lebedev Physical Institute, Russian Academy of Science (LPI RAS), Moscow, Russia
[d] Università di Bari, Bari, Italy
[e] Università di Bologna, Bologna, Italy
[f] Università di Cagliari, Cagliari, Italy
[g] Università di Ferrara, Ferrara, Italy
[h] Università di Genova, Genova, Italy
[i] Università di Milano Bicocca, Milano, Italy
[j] Università di Roma Tor Vergata, Roma, Italy
[k] Università di Roma La Sapienza, Roma, Italy
[l] AGH - University of Science and Technology, Faculty of Computer Science, Electronics and Telecommunications, Kraków, Poland
[m] LIFAELS, La Salle, Universitat Ramon Llull, Barcelona, Spain
[n] Hanoi University of Science, Hanoi, Viet Nam
[o] Università di Padova, Padova, Italy
[p] Università di Pisa, Pisa, Italy
[q] Università degli Studi di Milano, Milano, Italy
[r] Università di Urbino, Urbino, Italy
[s] Università della Basilicata, Potenza, Italy
[t] Scuola Normale Superiore, Pisa, Italy
[u] Università di Modena e Reggio Emilia, Modena, Italy
[v] Iligan Institute of Technology (IIT), Iligan, Philippines
[w] Novosibirsk State University, Novosibirsk, Russia [†]Deceased

JHEP11(2017)170